

Temporal dynamics of whole-brain networks across depths of unconsciousness

Dominic Standage (d.standage@bham.ac.uk)

School of Psychology, University of Birmingham, Hills Building, Birmingham, B15 2TT, UK

Corson N. Areshenkoff (c.areshenkoff@queensu.ca)

Centre for Neuroscience Studies, Queen's University, 18 Stuart St. Kingston, Ontario, K7L 3N6, Canada

Joseph Y. Nashed (jnashed@gmail.com)

Centre for Neuroscience Studies, Queen's University, 18 Stuart St. Kingston, Ontario, K7L 3N6, Canada

R. Matthew Hutchison (matthew.hutchison@biogen.com)

Biogen, 300 Binney St, Building 9, Fifth Floor, Cambridge, MA 02142, USA

Melina Hutchison (melina.hutchison@meei.harvard.edu)

Massachusetts Eye and Ear Infirmary, 243 Charles St, Boston, MA 02114, USA

Ravi S. Menon (rmenon@robarts.ca)

Robarts Research Institute, Western University, 1151 Richmond Street North, London, Ontario N6A 5B7, Canada

Stefan Everling (severlin@uwo.ca)

Robarts Research Institute, Western University, 1151 Richmond Street North, London, Ontario N6A 5B7, Canada

Jason P. Gallivan (gallivan@queensu.ca)

Centre for Neuroscience Studies, Queen's University, 18 Stuart St. Kingston, Ontario, K7L 3N6, Canada

Abstract

An understanding of consciousness is a long-standing goal of philosophy, neuroscience and medicine. A productive approach toward this goal is to investigate unconsciousness, through the use of general anaesthesia. Most investigations of this kind have focused on the effects of anaesthetics on cellular mechanisms, but it is unclear how these effects are manifest at the whole-brain level. We used resting-state functional magnetic resonance imaging (fMRI) to investigate the effects of the anaesthetic isoflurane on the dynamics of whole-brain network structure in macaque monkeys, following loss of consciousness. Analyses of the time-evolution of modular structure in these networks showed that higher isoflurane dose was associated with an increase in the number of modules, an increase in the uncoordinated movement of brain regions between modules, and an increase in the integration of brain networks derived from the modules. Conversely, higher dose was associated with a decrease in the coordinated movement of brain regions between modules and a decrease in intra-network connectivity. These results provide evidence for the fractionation and weakening of modular structure across depths of unconsciousness, and they take a step toward characterizing consciousness as an emergent property of whole-brain dynamics.

Keywords: Consciousness; anaesthesia; whole-brain functional networks; resting-state fMRI

Introduction

Consciousness has long been a focus of philosophers, neuroscientists and physicians alike, largely because of the broad implications of consciousness for our understanding of cognitive experience, but also because disruptions to consciousness are associated with neural pathologies and are often induced in clinical practice (anaesthesia). Indeed, our understanding of consciousness has been advanced in recent decades by the reversible induction of unconsciousness by general anaesthesia. Much of this research has focused on the cellular effects of anaesthetics, but it is unclear how these local effects are manifest as unconsciousness at the large-scale level (Franks, 2006; Alkire, Hudetz, & Tononi, 2006; Brown, Purdon, & Dort, 2011). Despite the common use of anaesthetics in clinical settings for surgical procedures, their effects on the properties of network-level brain activity are poorly understood. Here, we take a network neuroscience approach (Bassett & Sporns, 2017), using fMRI to examine the effects of the common anaesthetic isoflurane on measurements derived from the time-evolution of whole-brain network structure.

Network neuroscience analyses can be categorized as stationary or dynamic, where the former considers networks constructed from full neuroimaging scans, and the latter considers networks constructed from sliding time windows (temporal networks), allowing the measurement of network changes during scans. Earlier stationary analyses of the data addressed here showed that the strength of intra-network connectivity decreased with increasing isoflurane dose, while networks became more fractionated (more detected modules,



see below). Dynamic analysis identified fewer unique brain states with increasing dose, and fewer transitions between these states (Hutchison, Hutchison, Manning, Menon, & Everling, 2014). Here, we build on these findings, using methods that have been highly productive for investigating whole-brain dynamics in the performance of cognitive tasks [e.g. Bassett et al. (2011); Braun et al. (2015)]. The underlying assumption of these methods is that whole-brain networks are comprised of sub-networks or modules. Optimal modularity achieves a functional balance of dense within-module connectivity and sparse between module connectivity, trading off functional specialization and robustness with the computational power of integration over specialized systems [see e.g. Bassett et al. (2011)].

We tested three hypotheses. First, we sought to confirm that whole-brain networks would become more fractionated at deeper levels of unconsciousness under our sliding-window approach. Thus, we tested the hypothesis that the number of temporal modules will increase with isoflurane dose. Second, we reasoned that if the intra-connectivity of brain networks becomes weaker with increasing dose, then smaller perturbations (e.g. background noise) may be sufficient to drive small, random network reconfigurations, leading to uncoordinated changes in module membership. We therefore quantified the degree to which brain regions move between modules in a coordinated manner, testing the hypothesis that disjointed modular flexibility (Telesford et al., 2017) will increase with dose. Third, we sought to confirm that dynamic whole-brain structure would show weaker intra-network connectivity, as previously found with stationary analysis. Thus, we tested the hypothesis that the strength of interactions within networks (derived from modules) will decrease with increasing dose.

Methods

Functional and anatomical neuroimaging data were collected from five macaque monkeys (*Macaca fascicularis*; 4 females) on an actively shielded 7-Tesla horizontal bore scanner at the University of Western Ontario. An in-house designed and manufactured conformal 5-channel transceiver primate-head radiofrequency coil was used in all experiments. Following animal preparation, two functional scans were acquired at six increasing levels of isoflurane dose: 1.00, 1.25, 1.50, 1.75, 2.00, and 2.75%. Acquisition time on each scan was 5 min (Figure 1A). Each increase in dose was interleaved with a 10 min period to allow for the concentration to stabilize. The acquisitions of two anatomical images occurred during the stabilization periods between dose levels.

Functional image preprocessing was implemented in the FMRIB Software Library toolbox (FSL; <http://www.fmrib.ox.ac.uk>), consisting of motion correction, brain extraction, spatial smoothing, and high-pass and low-pass temporal filtering. Functional data were then registered to the F99 atlas template (Van Essen, 2004) and connectivity matrices were derived from a cortical parcellation of 174 (87 per hemisphere) cortical regions of interest (ROI), allowing the assess-

ment of large-scale patterns of functional connectivity and anaesthesia-induced changes (Figure 1B). Following regression of the average white matter, cerebral spinal fluid and six motion parameters from the time series, we calculated the mean time series of each ROI by averaging the time series across all voxels contained within it. Each ROI time series was then divided into windows of 60 seconds (30 imaging volumes) where contiguous windows overlapped by 50%. We constructed functional networks in each time window by calculating the Pearson correlation coefficient for each pair of ROIs (Figure 1C). All connections that did not pass false discovery rate correction (Benjamini & Yekutieli, 2001) were set to zero, as were all negative connections (a requirement of the module detection approach used). We determined the modular structure of the resulting multislice networks with a generalized Louvain method for time-resolved clustering (Jeub et al, <http://netwiki.amath.unc.edu/GenLouvain>, 2011-2017). This algorithm was repeated 100 times with random initialisation, resulting in 100 clustering solutions (a.k.a. partitions).

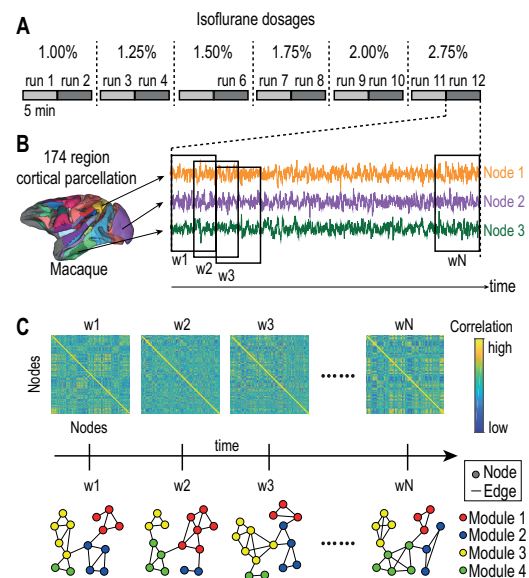


Figure 1: (A) Two 5 minute cans were conducted on each of six isoflurane dose levels. (B) Each subjects cerebrum was parcellated into 174 discrete brain regions and the average time series was extracted for each region (3 regions shown). The resulting time series were divided into 60s windows. (C) Correlation matrices were constructed in each time window, producing a multi-slice (temporal) network in each scan. Time-resolved clustering was used to detect modules in the temporal networks.

Results

The identified modules differed significantly from those derived from three established classes of null network for temporal modules, where the mean quality function of the real

networks was greater than that of the null networks [Figure 2A; see Bassett et al. (2011)]. For each subject and scan, we calculated the number of modules, as well as the flexibility of each ROI, defined as the number of times the ROI changed its module, relative to the number of possible changes (transitions between windows) (Bassett et al., 2011). We further calculated two sub-categories of flexibility, known as disjointedness and cohesion strength (Telesford et al., 2017), defined as the number of times an ROI changes modules by itself or with other ROIs respectively, relative to the number of possible changes. The mean number of modules and mean disjointedness across subjects both showed strong positive correlations with dose (Figure 2B,C), whereas cohesion strength showed a strong negative correlation with dose (Figure 2D). These results were extremely robust across window size, window step, network threshold (e.g. uncorrected networks and FDR-corrected networks) and the resolution of time-resolved clustering.

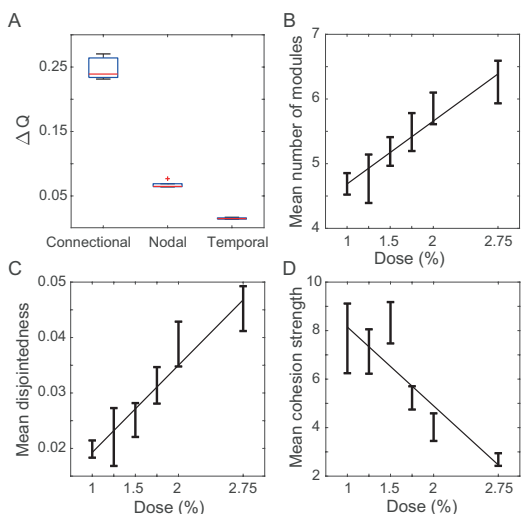


Figure 2: (A) Subjects' whole-brain networks showed significant temporal modular structure compared to three classes of null network. Boxplots show differences in mean modularity ΔQ between real and permuted networks for connectional (one-sample t-test; $t=31.55$, $p=6.01e-6$), nodal ($t=27.97$, $p=9.72e-6$) and temporal ($t=27.28$, $p=1.07e-5$) null models. Means were taken across all dose levels. (B) Mean number of modules for each level of isoflurane dose. Means were first taken over both scans for each dose, and then taken over all subjects. Error bars show standard error. Pearson's $r=0.98$. Thin line shows least squares linear fit. (C) Mean disjointedness for each dose ($r=0.98$). (D) Mean cohesion strength for each dose ($r=-0.90$).

To investigate whether isoflurane influenced the intra-connectivity of brain networks and the degree to which these networks interact with one another, we determined the proportion of modular partitions (across all subjects and scans) in which each pair of ROIs was placed in the same mod-

ule, referred to as a module allegiance matrix (Bassett, Yang, Wymbs, & Grafton, 2015). We then used non-negative matrix factorization to cluster the edges of this matrix, identifying four clusters that correspond to whole-brain networks. We took this approach to network identification because of the known degeneracy of the generalized Louvain algorithm used here, i.e. very different partitions can have nearly identical quality function scores [see Bassett et al. (2011)]. Thus, our clustering approach effectively identified a consensus modularity partition. These four networks are shown in Fig 3A.

With each ROI assigned to a network, the interaction between any two networks was measured by $I_{k1,k2} = (\sum_{i \in C_{k1}, j \in C_{k2}} P_{i,j}) / (|C_{k1}| |C_{k2}|)$ (Bassett et al., 2015), where $C_{k \in 1,2}$ are modules, $|C_k|$ is the number of ROIs they contain, and $P_{i,j}$ is the proportion of the time ROIs i and j are in the same module. Self-interaction [referred to as recruitment in the task-based analysis by Bassett et al. (2015)] is calculated by allowing $k1 = k2$. The integration between two modules $k1 \neq k2$ is the normalized interaction strength between them, calculated as $I'_{k1,k2} = I_{k1,k2} / \sqrt{I_{k1,k1} I_{k2,k2}}$.

An analysis of variance showed strong main effects of dose ($f=9.63$, $p=0$) and network ($f=12.84$, $p=0$) on self-interaction, and a strong interaction between dose and network ($f=2.08$, $p=0.0012$). For three out of four networks, there was a strong positive correlation between dose and self-interaction (Figure 3B left). There were strong main effects of dose ($f=11.37$, $p=0$) and network ($f=16.77$, $p=0$) on the mean integration of each network with the other networks, and a strong interaction between dose and network ($f=2.15$, $p=0.0008$). The same three networks that showed decreasing self-interaction with increasing dose showed increasing mean integration with dose (Figure 3B right). Dose did not affect self-interaction or mean integration in the remaining network, comprised of visual and somatomotor areas (Figure 3A).

Summary

Our temporal module analysis found that whole-brain networks became more fractionated and weakly connected at deeper levels of unconsciousness. In this regard, dose was positively correlated with the number of modules detected (Figure 2B), and the strength of connectivity within three out of four networks derived from the modules decreased with increasing dose, as measured by the self-interaction of these networks (Figure 3B left). Furthermore, we found that as self-interactions decreased, the mean integration of the same three networks increased (Figure 3B right), quantifying a general decrease of structure at the whole-brain level. Our finding that mean disjointedness increased at deeper levels of unconsciousness (Figure 2C) is consistent with our hypothesis that weaker network structure should lead to more haphazard, uncoordinated modular changes, and our finding that cohesion strength decreased with dose (Figure 2D) is consistent with the reduction of whole-brain state transitions at higher isoflurane dose reported by Hutchison et al. (2014), assuming that such state transitions are more readily driven by groups of

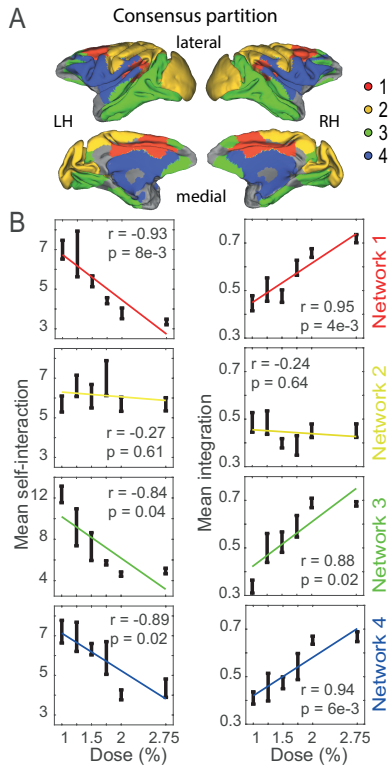


Figure 3: (A) Clustering of the module allegiance matrix over all subjects and scans produced a consensus modular partition, consisting of a cingulo-parieto-frontal network (Network 1, red), a visual and somatomotor network (Network 2, yellow), a ventrotemporal-prefrontal network (Network 3, green) and a lateral parieto-frontal cingulate temporal network (Network 4, blue). (B) Mean self-interaction (left) and integration (right) of each network for each isoflurane dose. Means were taken over both scans for each dose, and then over all subjects. Error bars show standard error. Lines show least squares linear fit.

brain regions acting in concert than by individual brain regions. Future work should address this possibility. Overall, our study further characterizes the whole-brain dynamics of anaesthesia-induced unconsciousness, and by extension, takes a step toward the long-standing goal of a mechanistic understanding of consciousness.

References

- Alkire, M. T., Hudetz, A. G., & Tononi, G. (2006). Consciousness and anesthesia. *Science*, *322*, 876–880.
- Bassett, D. S., & Sporns, O. (2017). Network neuroscience. *Nature Neuroscience*, *20*, 353–364.
- Bassett, D. S., Wymbs, N. F., Porter, M. A., Mucha, P. J., Carlson, J. M., & Grafton, S. T. (2011). Dynamic reconfiguration of human brain networks during learning. *Proceedings of the National Academy of Sciences of the United States of*

- America*, *108*, 7641–7646.
- Bassett, D. S., Yang, M., Wymbs, N. F., & Grafton, S. T. (2015). Learning-induced autonomy of sensorimotor systems. *Nature Neuroscience*, *18*, 744–751.
- Benjamini, Y., & Yekutieli, D. (2001). The control of the false discovery rate in multiple testing under dependency. *The Annals of Statistics*, *29*, 1165–1188.
- Braun, U., Schafer, A., Walter, H., Erk, S., Romanczuk-Seiferth, N., Haddad, L., ... Bassett, D. S. (2015). Dynamic reconfiguration of frontal brain networks during executive cognition in humans. *Proceedings of the National Academy of Sciences of the United States of America*, *112*, 11678–11683.
- Brown, E. N., Purdon, P. L., & Dort, C. J. V. (2011). General anesthesia and altered states of arousal: A systems neuroscience analysis. *Annual Review of Neuroscience*, *34*, 601–628.
- Franks, N. P. (2006). Molecular targets underlying general anaesthesia. *British Journal of Pharmacology*, *147*, 72–81.
- Hutchison, R. M., Hutchison, M., Manning, K. Y., Menon, R. S., & Everling, S. (2014). Isoflurane induces dose-dependent alterations in the cortical connectivity profiles and dynamic properties of the brain's functional architecture. *Human Brain Mapping*, *35*, 5754–5775.
- Telesford, Q. K., Ashourvan, A., Wymbs, N. F., Grafton, S. T., Vettel, J. M., & Bassett, D. S. (2017). Cohesive network reconfiguration accompanies extended training. *Human Brain Mapping*, *38*, 4744–4759.
- Van Essen, D. C. (2004). Surface-based approaches to spatial localization and registration in primate cerebral cortex. *NeuroImage*, *23*, S97–S107.